Dicle University
Journal of Engineering
https://dergipark.org.tr/tr/pub/dumf
duje.dicle.edu.tr

Research Article

Explainable Boosting Machine-Based Analysis of Delay at Signalized Intersections

Ruti POLİTİ[1*]

[1] Izmir University of Economics, Civil Engineering Department, ruti.politi@ieu.edu.tr, Orcid No: 0000-0001-7851-2506

ARTICLE INFO

Article history:

Received 1 February 2026
Received in revised form 13 July 2026
Accepted 14 July 2026
Available online 7 August 2026

Keywords:

signalized intersection, control delay, explainable boosting machine, data-driven modeling, predictive modeling

Doi: 10.24012/dumf.1879464

* Corresponding author

ABSTRACT

Urban traffic signal control plays an important role in improving operational efficiency and reducing unnecessary delays in transportation networks. However, capturing the complex nonlinear relationships between traffic demand and signal timing parameters remains a major challenge under varying operating conditions. This study proposes an explainable artificial intelligence (XAI) framework for traffic signal delay analysis using scenario-driven operational data from a three-leg signalized intersection. An Explainable Boosting Machine (EBM) was developed to model the relationships between cycle time, phase split, arrival flow, and intersection delay, and was comparatively evaluated against Random Forest (RF) and XGBoost models using 5-fold cross-validation. The EBM model achieved high predictive performance (R^2 = 0.89, RMSE = 1.94), while simultaneously providing transparent interpretation of variable effects through global importance analysis, shape functions, and pairwise interactions. The results indicate that cycle time and phase allocation are among the key factors influencing delay formation, with nonlinear interaction patterns observed under different traffic demand conditions. An interaction was observed between cycle length and Phase C allocation (north approach turning phase), suggesting a condition-dependent relationship with delay. Comparative analyses further demonstrated a general consistency between EBM and benchmark ensemble models in identifying influential operational variables. The proposed framework provides predictive capability and interpretable insights that may support data-driven traffic signal analysis and operational decision-making.

Introduction

Signalized intersections, as critical control points within road networks, play an important role in shaping traffic performance. Inefficient signal timing leads not only to increased delay and queue formation but also to unnecessary fuel consumption and emissions, reflecting the loss of system efficiency [1]. Recent advances in data-driven modeling and artificial intelligence (AI) provide new opportunities to analyze traffic signal performance beyond traditional performance indicators. Machine learning (ML)-based approaches can effectively represent nonlinear relationships between traffic flow, control parameters, and resulting delay [2]. The integration of interpretability into data-driven traffic signal models offers an opportunity to support more informed decision-making [3].

This study proposes an explainable artificial intelligence (XAI) framework based on Explainable Boosting Machine (EBM) for traffic signal control. By modeling signalized intersection average control delay as an indicator of system inefficiency, the study aims to both predict intersection performance and reveal the underlying influence of key traffic and signal parameters. The use of EBM enables the decomposition of delay into additive and interaction effects within a glass-box framework, allowing transparent interpretation of variable contributions while maintaining predictive performance. Through global feature importance, shape functions, and pairwise interaction analyses, the proposed framework provides insights into how traffic demand and signal timing variables influence delay formation under varying operating conditions. This interpretability may support data-driven decision-making in urban traffic management by improving the understanding of model behavior.

Literature Review

Average control delay is a fundamental performance indicator in traffic engineering and is widely used to evaluate the operational efficiency of signalized intersections. It represents the cumulative effects of vehicle deceleration, stopping, queueing, and acceleration experienced during signalized control [4]. Traditional delay estimation approaches, including Highway Capacity Manual (HCM), [5], Webster's formulation [6] and Akçelik's model [7], relate delay to operational characteristics such as traffic demand, cycle length, green time ratio, and degree of saturation. Vehicle delay at signalized intersections has been the subject of numerous modeling studies [8-11]. These studies similarly highlight the strong influence of signal control parameters on delay performance. However, the relationships among these variables are often nonlinear and vary across operating conditions, making it challenging to fully represent complex traffic dynamics [12, 13].

Previous research on traffic signal control has evolved from analytical delay models toward machine learning-based approaches, where early applications of artificial intelligence demonstrated the ability to capture nonlinear relationships between traffic conditions and delay. Murat [14] compared fuzzy logic and artificial neural network models for vehicle delay estimation and reported that both approaches provided satisfactory predictive performance under signalized traffic conditions. Similarly, Murat and Baskan [10] developed an artificial neural network-based framework for modeling vehicle delays at signalized junctions, highlighting the capability of AI techniques to capture nonlinear traffic relationships. These studies contributed to the development of AI-based delay modeling and provided a foundation for subsequent machine learning applications in traffic engineering.

More recent studies have focused on improving both predictive performance and interpretability through advanced machine learning and explainable AI techniques [3]. EBM has been successfully applied in various engineering domains such as material strength prediction in concrete composites [15], compressive strength modeling of sustainable mortar [16], and environmental morphology studies [17], demonstrating both high predictive performance and interpretability. For travel time prediction studies, Ahmed, et al. [18] applied SHapley Additive Explanations (SHAP) analysis to explain the effects of spatio-temporal features on travel time estimations. Zhang [19] applied tree-based machine learning models to traffic flow prediction and evaluated their interpretability through feature importance analysis, showing consistency with observed traffic patterns. Alahmadi, et al. [20] employed an EBM to model work zone crash severity using crash data and demonstrated that EBM provides competitive performance relative to black-box models while offering global and interaction-level interpretations. Liu, et al. [21] introduced a genetic programming-based signal control algorithm that automatically generates descriptive rules for phase switching, advancing interpretable traffic signal control methodologies. Similarly, Santhiya, et al. [22] applied the local interpretable model- agnostic explanation (LIME) algorithm to traffic signal detection tasks to enhance the model decision tasks. Erten and Gürfidan [23] employed regression-based ensemble machine learning models to predict Marshall stability and flow values of hot-mix asphalt mixtures. Model interpretability was enhanced through SHAP analysis, which identified key material and volumetric parameters influencing asphalt performance. While post-hoc interpretability methods have been widely used to analyze machine learning models [24], EBM provides an additive modeling framework that allows direct examination of individual feature effects and pairwise interactions, which can be advantageous for traffic signal performance analysis.

While earlier studies demonstrated the effectiveness of ML techniques for traffic delay prediction, recent research has increasingly emphasized model interpretability in addition to predictive performance. In this context, the proposed framework combines delay prediction with an interpretable analysis of variable importance, and pairwise interactions using the EBM approach.

Methodology

The study presents a data-driven and explainable modeling framework to analyze traffic signal performance under varying demand and signal timing conditions. The overall workflow consists of (i) scenario generation for signalized intersection, (ii) modeling with SIDRA-based simulation to extract the operational performance indicators, (iii) calibration and validation, and (iv) development of an explainable machine learning model to quantify the influence of signal control and traffic-related parameters on delay prediction.

Scenario Generation and Data Set

A three-leg signalized intersection was modeled using SIDRA Intersection (version 6.1) software, a widely used traffic simulation and analytical software for evaluating intersection performance and assessing the impacts of alternative operational scenarios [25].

A total of 50 scenarios were generated with traffic volumes ranging from 1400 to 3800 veh/h. The scenario set was designed to ensure a balanced distribution across low, medium, and relatively high demand levels. A reference traffic volume matrix was initially established based on representative traffic conditions at the analyzed signalized intersections. Using this reference matrix, traffic demand levels were changed to generate alternative operating scenarios. The resulting 50 scenarios were categorized into low, medium, and high demand conditions according to the total intersection traffic volume. Total traffic volumes between 1400-2500 veh/h were classified as low demand, volumes between 2500-3000 veh/h as medium demand, and volumes above 3000 veh/h as relatively high demand [1].

A base saturation flow rate of 1950 veh/h/lane [26] was adopted, consistent with the default SIDRA configuration and values reported in previous traffic engineering studies [9, 26, 27]. This assumption provides a basis for evaluating the effects of traffic demand and signal timing parameters on delay under different operating scenarios.

Modeling with SIDRA Intersection

SIDRA provides a widely used simulation-based framework for representing signalized intersection operations under controlled traffic conditions and is commonly used in traffic engineering studies for performance evaluation [28].

The simulation outputs were organized into a structured dataset for XAI analysis. The dependent variable was defined as average control delay (s/veh), representing intersection performance. The input features include key explanatory variables commonly used in traffic engineering, such as traffic volume, cycle length, arrival flows, and phase split ratios. Phase split in SIDRA refers to the allocation of the signal cycle among individual phases, defined by the green and intergreen times assigned to each phase. It is typically expressed as a proportion of the total cycle length [29].

The analyzed intersection geometry includes a short approach leg with an exclusive left-turn lane, as illustrated in Figure 1. This geometric configuration was considered in the scenario design, as it affects queue formation, signal phase allocation, and operational delay, which is referred to as the SIDRA-based model.

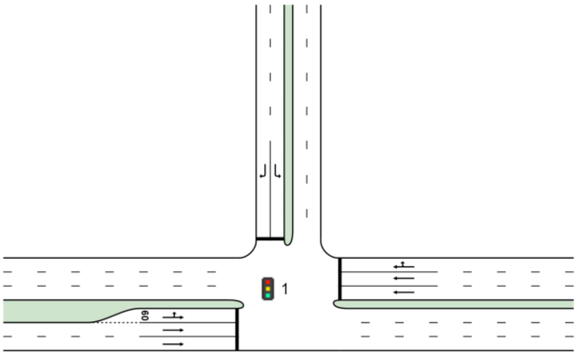

Figure 1. Schematic layout of the analyzed three-leg signalized intersection of SIDRA-based model.

The intersection operated under a three-phase fixed-time signal control scheme, with cycle lengths varying between 50 and 120 seconds, as illustrated in Figure 2. Phase A represents the west-approach movements (through and left turn), Phase B controls through movements in both eastbound and westbound directions, and Phase C is dedicated to north approach, including north-to-east and north-to-west turning movements.

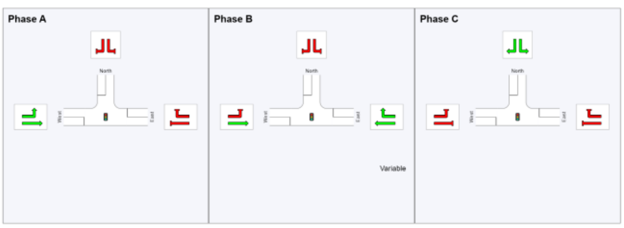

Figure 2. Three-phase signal control structure used in the SIDRA-based model.

The selected cycle length ranges and signal timing settings were determined based on commonly adopted traffic engineering practice, HCM framework, and previous delay studies at signalized intersections [1, 5, 30-32]. The generated scenarios were designed to represent varying traffic demand and operational conditions for delay analysis.

The intergreen parameters were kept constant across all scenarios, with a yellow time of 4 s [33] and an all-red time of 2 s [26, 34] for each phase. These values were adopted from the default SIDRA settings and are consistent with commonly used signal timing practices reported in previous studies.

Calibration and Validation

In the SIDRA-based model framework, calibration and validation were performed using empirical traffic data from two intersections in Karşıyaka, İzmir, Turkey. The intersections share similar geometry and traffic characteristics and operate under actuated control with a 70 s cycle time. The field observations were used solely to calibrate and validate the SIDRA simulation model, whereas the EBM model was trained and tested using the scenarios generated by the calibrated SIDRA model.

Traffic data were extracted from video recordings under good weather conditions (clear visibility, no wind, and no weather-related disruptions) during the morning peak period (7:30-8:30 AM). Vehicle movements were recorded using two cameras at each intersection, and queue lengths were estimated at 5 min intervals based on the last vehicle position during the red phase, following the methodology in [35, 36].

Local traffic flow parameters and observed signal timings were incorporated into the SIDRA-based model through calibration of the Area Type Factor (ATF), ranging from 0.1 to 2 and was calculated using the empirical formulation (Equation (1)) proposed by Bozkurt and Çalışkanelli [37]. The ATF was applied to all approaches based on total traffic volume (V_{Total}), right-turn rate (RT), and left-turn rate (LT) [37, 38].

$$ATF = 0.0013 * V_{Total} - 2.23488 * RT - 22.8015 * LT \tag{1}$$

Model calibration and validation were conducted using field-observed traffic data and SIDRA simulation outputs in a comparison framework based on the Geoffrey E. Havers (GEH) statistic [39]. GEH is a widely used traffic engineering measure for evaluating the agreement between observed and modeled traffic volumes [25, 28, 34, 40]. GEH statistic, defined in Equation (2), evaluates the consistency between modeled traffic volumes (M) and volumes obtained from simulation-based observations (O) [41]. In traffic engineering applications, GEH values below 5 are generally considered to indicate an acceptable level of agreement between observed and modeled traffic volumes [28].

$$GEH = \sqrt{\frac{2(M-O)^2}{M+O}} \tag{2}$$

Table 1 summarizes the average GEH values for the morning peak hour. All approach-level GEH values were below the acceptable threshold of 5, with an average GEH of 1.89, indicating good agreement between simulated and observed traffic conditions. Regarding GEH evaluation, the westbound right (WBR), westbound left (WBL), northbound through (NBT), northbound right (NBR), southbound through (SBT), and southbound left (SBL) movement approaches yielded GEH values below the acceptable threshold of 5.

Table 1. GEH values according to the number of vehicles in a queue.

Intersection No	Approach	GEH Statistic
1	WBR	2.1518
	NBT	0.1094
	NBR	0.1094
	SBT	0.1407
2	WBL	3.8497
	WBR	3.1300
	NBT	2.1783
	NBR	2.9192
	SBL	3.8025
	SBT	0.4650
The avg. value of GEH:		**1.8856**

Machine Learning Models

A data-driven modeling approach is adopted to capture the complex relationships between traffic demand, signal control parameters, and intersection performance. This approach uses machine learning techniques to learn system behavior from operational data [2]. EBM was employed to model the relationship between signal control parameters, traffic demand characteristics, and intersection delay.

EBM is an interpretable, glass-box machine learning model built on generalized additive models (GAMs) [20]. The model represents the predicted outcome as a sum of individual feature effects and, when included, pairwise interaction terms [42]. This generalized additive model combines the predictive strength of ensemble learning with interpretable structure [20]. In addition to predictive accuracy, the model provides explanations of how each parameter contributes to delay formation through global feature importance [43] and shape functions [44]. Global explanation (feature importance plot) quantifies the overall contribution of each predictor to the model's output across the dataset by averaging the effect magnitude of its learned function [45], while shape functions visualize how individual feature values relate to predicted outcomes, revealing the direction and strength of each variable's influence [44].

A sensitivity analysis was conducted to assess the effectiveness of the EBM model with respect to key hyperparameters [20, 42]. Three alternative configurations were tested in addition to the default model with testing learning rates from the literature [20], and keeping other settings constant.

To provide a comparative evaluation of the proposed EBM framework, Random Forest (RF) and Extreme Gradient Boosting (XGBoost) models were additionally implemented as benchmark machine learning approaches. RF is an ensemble tree-based learning method [13] that improves prediction accuracy through aggregation of multiple decision trees [46], while XGBoost is a gradient boosting framework widely used for nonlinear regression problems and structured datasets [47]. Feature importance analysis was employed to quantify the relative contribution of each input variable to the predictive performance of the machine learning models [48]. Hyperparameter tuning for all models was conducted using GridSearchCV with 5-fold cross-validation (CV) based on parameter ranges commonly adopted in previous studies [13, 48-53].

Model Evaluation and Explainability Analysis

Model performance was evaluated using standard regression metrics, including the coefficient of determination (R^2) (Equation (3)), root mean square error (RMSE) (Equation (4)), and mean absolute error (MAE) (Equation (5)), which measure the average deviation between predicted and observed values [12, 54]. In addition to predictive performance comparisons among the evaluated machine learning models, explainability analysis was conducted for the EBM framework through global feature importance scores and feature-specific shape functions [44]. In all equations, n gives the number of observations, y_i denotes the observed, z_i shows the predicted delay values, and $\bar{y}$ represents the mean observed delay [12].

$$R^2 = 1 - \frac{\sum_{i=1}^{n}(y_i - z_i)^2}{\sum_{i=1}^{n}(y_i - \bar{y})^2} \tag{3}$$

$$RMSE = \sqrt{\frac{\sum_{i=1}^{n}(y_i - z_i)^2}{n}} \tag{4}$$

$$MAE = \frac{1}{n}\sum_{i=1}^{n}(y_i - z_i) \tag{5}$$

Results and Discussion

The proposed XAI model demonstrates strong predictive performance in estimating intersection delays based on traffic demand and signal control parameters. The results confirm the capability of data-driven approaches to capture the nonlinear and interactive effects in signalized intersection operations.

Hyperparameter Tuning of ML Models

Hyperparameter tuning for all machine learning models was conducted using a 5-fold cross-validation. All machine learning models were implemented in Python 3.13. A representative set of grid search parameter combinations was evaluated to ensure computational efficiency and methodological consistency across models [48].

The EBM model was tested under four learning rates (0.01 as default, 0.03, 0.05, 0.1) with max_bins of 32 (Table 2). The results indicate that the configuration with a $learning\_rate$ of 0.1 provides the best balance between accuracy, achieving the highest R^2 (0.886) and the lowest RMSE (1.937) and MAE (1.299). The other configurations showed slightly lower R^2 and higher errors, confirming that the default parameters are suitable for the analysis.

For RF model, the tuning process was considered with the number of trees ($n\_estimators$ = 100, 200) and maximum tree depth (max_depth = 5, 10). The results of the hyperparameter combinations are presented in

Table 3.

Table 2. Hyperparameter tuning results of EBM.

Model	learning_rate	max_bins	RMSE	MAE	R^2
LR001	0.01	32	1.9669	1.3409	0.8830
LR003	0.03	32	1.9680	1.3617	0.8828
LR005	0.05	32	1.9539	1.3280	0.8845
LR01	**0.1**	**32**	**1.9369**	**1.2987**	**0.8864**

Table 3. Hyperparameter tuning results of RF.

Model	n_estimators	max_depth	RMSE	MAE	R^2
RF1	100	5	2.2943	1.6964	0.8407
RF2	100	10	2.2420	1.6415	0.8479
RF3	200	5	2.2403	1.6515	0.8481
RF4	**200**	**10**	**2.2063**	**1.6240**	**0.8527**

For the XGBoost (XGB) model, the tuning process included the number of trees ($n\_estimators$ = 100, 200), and maximum tree depth (max_depth = 3, 5) with a learning rate of 0.05 based on previous studies recommending values (0.01-0.1) for stable performance [48, 55]. The corresponding performance results are summarized in Table 4. The best-performing configuration for each model, highlighted in bold, was selected as the optimal set of hyperparameters based on the average cross-validation performance.

Table 4. Hyperparameter tuning results of XGBoost.

Model	n_estimators	max_depth	RMSE	MAE	R^2
XGB1	**100**	**3**	**2.0793**	**1.5147**	**0.8692**
XGB2	100	5	2.4607	1.9044	0.8168
XGB3	200	3	2.0756	1.5384	0.8690
XGB4	200	5	2.4782	1.9315	0.8142

The optimal hyperparameter configurations for each model were selected based on the minimum RMSE criterion and used in subsequent predictive performance and explainability analyses (Table 5).

Table 5. Selected optimal hyperparameters.

Model	Final Parameters
EBM	learning_rate = 0.1, max_bins = 32
RF	n_estimators = 200, max_depth = 10
XGBoost	n_estimators = 100, learning_rate = 0.05, max_depth = 3

Predictive Performance Comparison of ML Models

Model performances were assessed to evaluate the ability of the proposed framework and to predict signalized intersection control delay under varying traffic demand and signal timing conditions. Figure 3a-c presents the relationship between predicted and observed values for the EBM, RF and XGBoost models, respectively. The red dashed line indicates the 1:1 reference line. The EBM model achieved the highest predictive performance (R^2 = 0.886), followed by XGBoost (R^2 = 0.869) and RF (R^2 = 0.853). The close agreement between predicted and observed values demonstrates that all three models captured the nonlinear relationships between signal timing parameters, traffic demand, and intersection delay.

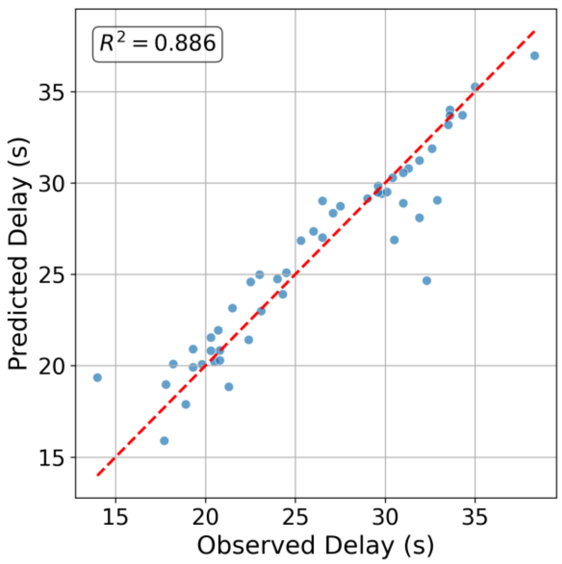

(a)

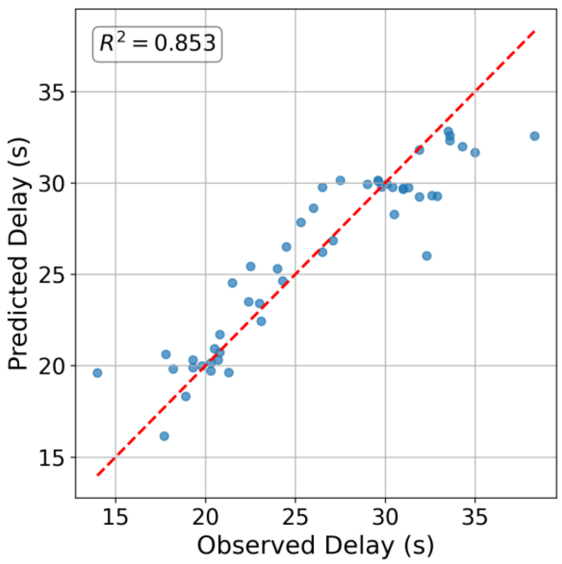

(b)

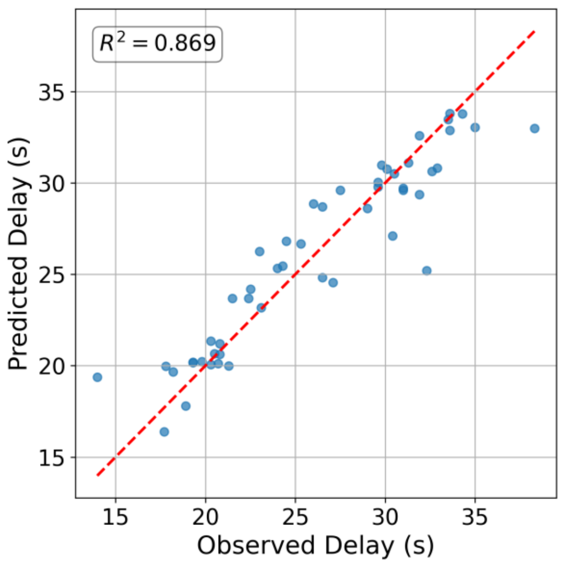

(c)

Figure 3. Predicted vs observed delay values for (a) EBM model, (b) RF model, and (c) XGBoost model.

The RF and XGBoost models also exhibit good predictive performance, confirming that ensemble-based learning methods are capable of modeling nonlinear relationships between traffic demand, signal control parameters, and delay. However, EBM framework provides additional interpretability while maintaining comparable accuracy. Although the proposed models achieved satisfactory predictive performance, their generalizability to a wider range of traffic conditions would benefit from further validation, highlighting the need for larger and more diverse simulation datasets as well as real-world observations.

Explainability Analysis of EBM Model

The comprehensive interpretation of the EBM model allows for an assessment of the impact of individual traffic and signal control factors on the predicted intersection delays. Figure 4 presents the contribution of each predictor to the model represented with global feature importance rankings obtained from the EBM model. Cycle time was identified as the most influential variable affecting intersection delay, followed by Phase Split B and Phase Split C. These findings suggest that delay formation is influenced primarily by signal timing decisions than demand alone within the examined operating conditions. In particular, the cycle time plays a key role in balancing green utilization and vehicle waiting times across competing movements. Similarly, green allocation effects vary across phases, indicating phase-specific sensitivity in delay formation. The findings confirm the importance of phase split allocations, indicating that the distribution of green time among phases is a key determinant of intersection performance. The explainability results align with established traffic engineering principles while offering additional quantitative insights.

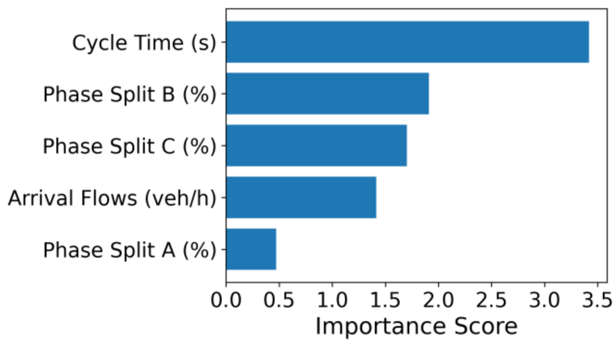

Figure 4. Global importance of signal timing and demand variables obtained from EBM.

To further assess the reliability of the EBM explanations, feature importance results were compared with those obtained from the RF and XGBoost models (Figure 5a and Figure 5b). A consistent pattern was observed between the EBM global importance rankings and the RF feature importance results, where cycle time and Phase Split B emerged as the dominant factors influencing delay. Although XGBoost assigned relatively greater importance to Phase Split C, indicating certain model-specific sensitivities to nonlinear traffic conditions, the overall ranking pattern remained broadly consistent across the three models. Overall, the key factors identified by EBM are supported by alternative ensemble learning approaches.

EBM-derived shape functions illustrate the marginal effects of each factor on average control delay. Shape functions capture nonlinear relationships between predictors and the response variable and visualize the threshold-based effects [56] of green split allocation on control delay, providing interpretable decision logic beyond the performance metrics. The shape function represents a one-dimensional relationship between a predictor variable and its corresponding contribution to the model output. Predictor values are shown on the horizontal axis, while the vertical axis represents the corresponding contribution scores [20], where positive and negative values represent increasing and decreasing effects on the predicted outcome, respectively [42]. Since the model output represents control delay, negative shape function scores indicate delay-reducing effects, whereas positive scores correspond to increased predicted delay. Values close to zero represent a reference effect with no substantial contribution relative to the average behavior.

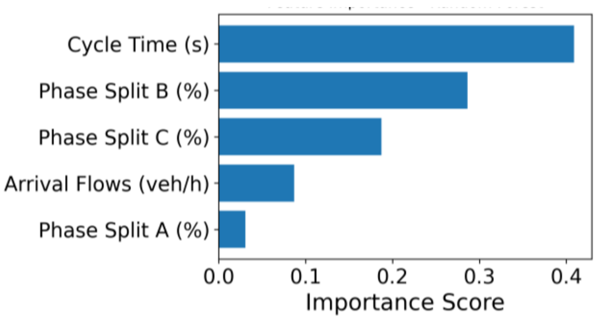

(a)

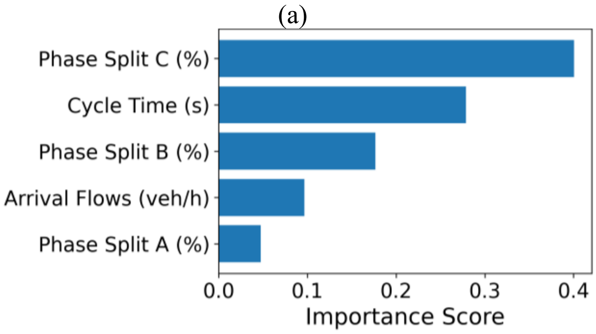

(b)

Figure 5. Comparison of variable importance rankings: (a) RF feature importance, (b) XGBoost feature importance.

Figure 6 represents the EBM shape function for cycle time, illustrating its relationship with average control delay. Short cycle times (below approximately 70 s) exhibit a negative contribution score, indicating improved operational performance and lower delay levels. Cycle lengths exceeding approximately 90-95 s exhibit positive contribution scores, indicating that longer cycles may increase vehicle waiting times and reduce overall intersection efficiency. Rather than indicating a single optimum cycle length, the results suggest the existence of a favorable operating range in which delay remains relatively low.

Figure 7 presents the effect of Phase A on control delay derived from the EBM model. Phase A exhibits a relatively limited impact on control delay compared to other phases. Green split ratios (below approximately 26% and above approximately 40%) are associated with lower predicted delay contributions under the observed operating conditions. Within the intermediate range (approximately 35-38%), the effect remains close to neutral, suggesting that Phase A is not a critical phase under the examined demand conditions. This effect needs to be interpreted together with the interactions between phase allocation and cycle length.

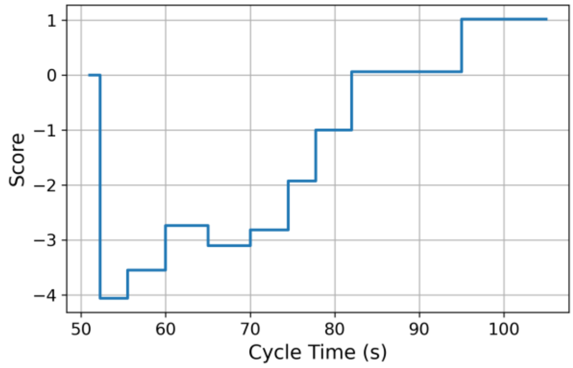

Figure 6. Shape function of cycle time on average control delay.

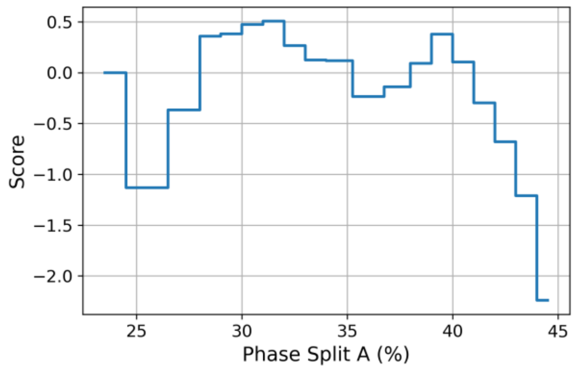

Figure 7. Shape function of green split allocation for Phase A on average control delay.

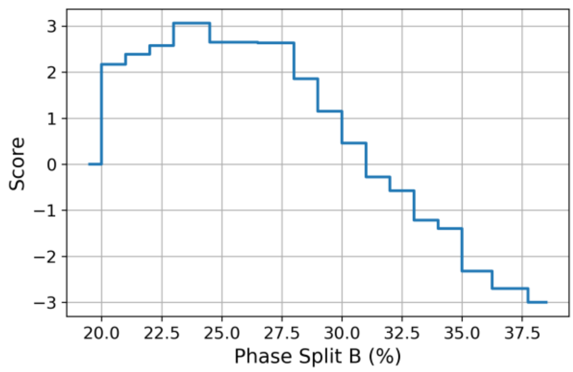

Figure 8. Shape function of green split allocation for Phase B on average control delay.

In contrast, Phase B (Figure 8) demonstrates a strong decreasing trend, where increasing green split ratios consistently reduces control delays. Lower green split allocations (below approximately 25%) significantly increase delay, while increasing the green split beyond 30% results in a delay reduction. This indicates that Phase B plays a dominant role in overall intersection performance and functions as the primary capacity-constraining movement group. Increasing green time allocation to the dominant east-west movements is generally associated with lower delay levels.

For Phase C (Figure 9), delay decreases as the green split increases from approximately 25% to 45%, reaching its minimum contribution within this range, indicating improved operational performance. However, further increases beyond 45% reverse this trend and lead to rapidly increasing delay contributions. This pattern suggests the existence of an optimal allocation range, beyond which additional green time allocated to Phase C may reduce the service capacity available for other phases and increase overall delay. Finally, arrival flow effects (Figure 10) indicate that delay remains relatively insensitive to demand variations at lower arrival flow levels. However, a noticeable increase in contribution scores is observed beyond approximately 3000 veh/h, suggesting that the intersection becomes increasingly sensitive to additional demand under higher traffic volumes. This confirms that delay is sensitive to demand fluctuations under higher volume conditions.

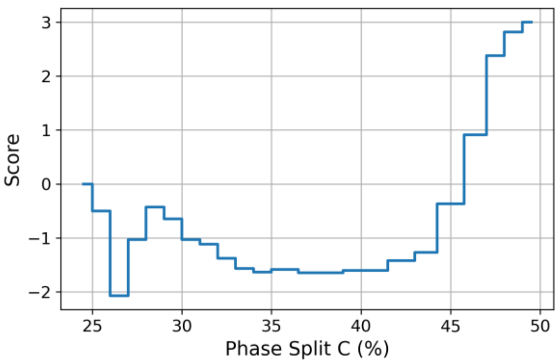

Figure 9. Shape function of green split allocation for Phase C on average control delay.

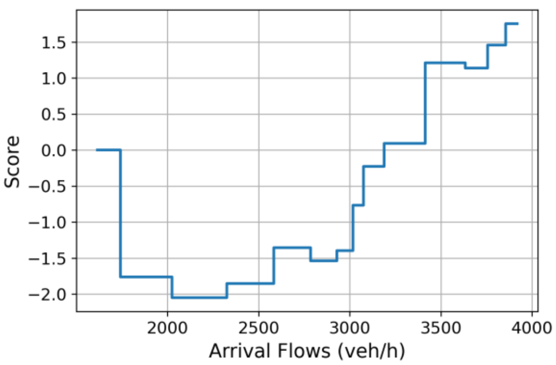

Figure 10. Shape function of arrival flow on average control delay.

EBM reveals context-dependent interaction mechanisms among traffic demand and signal control variables. In addition to main effects, pairwise interaction terms were incorporated into the model to capture the combined effect of traffic demand and signal control parameters. The interaction importance analysis, shown in Figure 11, revealed that interactions involving cycle time exhibited the strongest contribution to delay variability. Accordingly, interaction heatmaps were presented for the two most influential interaction terms identified by the importance analysis.

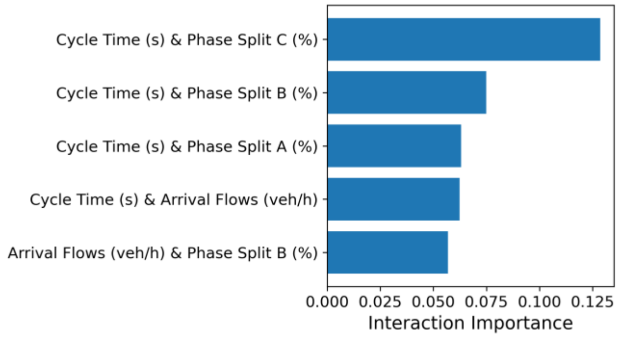

Figure 11. Feature importance plot of pairwise interactions.

To further investigate interaction structure among the most influential predictors, pairwise interactions identified by the EBM model were examined using two-dimensional heatmaps, as presented in Figure 12a-d. The color gradient from dark purple to bright yellow represents increasing interaction strength, reflecting a joint contribution of the corresponding variable pairs to the predicted control delay.

Figure 12a illustrates that the effect of Phase Split C on delay is dependent on cycle length, indicating a clear interaction between phase allocation and signal timing. Under short cycle conditions, variations in Phase Split C have a limited impact on delay, whereas under long cycle conditions, the increase in green allocation results in more pronounced delay contributions. Increasing the green time for Phase C requires redistributing effective green time from the major arterial phases serving through movements. Since Phase C primarily accommodates turning movements from the north approach, excessive allocation to this phase may reduce the available capacity for dominant through traffic streams, resulting in higher overall control delay. In particular, delay increased substantially when cycle lengths exceeded approximately 105 s in combination with Phase C allocations above 45%, highlighting the importance of jointly considering cycle length and phase allocation.

As shown in Figure 12b, unlike Phase C, increasing the green share allocated to Phase B generally reduces delay, particularly under long-cycle conditions. The interaction planes indicate that the highest delay contributions (bright yellow zones) occur when long cycle lengths (>105 s) combined with low green splits (<22%) correspond to operationally unstable conditions characterized by insufficient capacity for dominant east-west through movements. This can lead to rapid queue accumulation and reduced discharge efficiency, suggesting that Phase B plays an important role in accommodating major traffic movements.

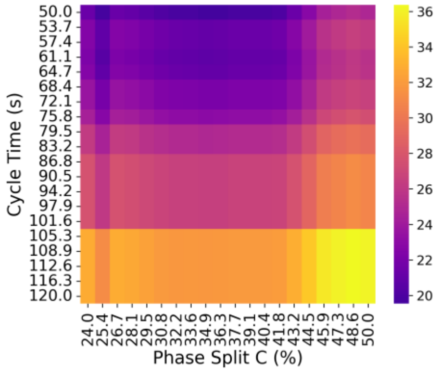

(a)

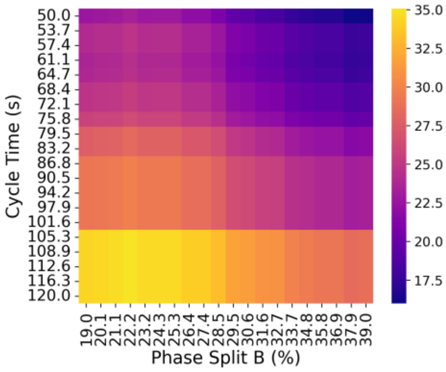

(b)

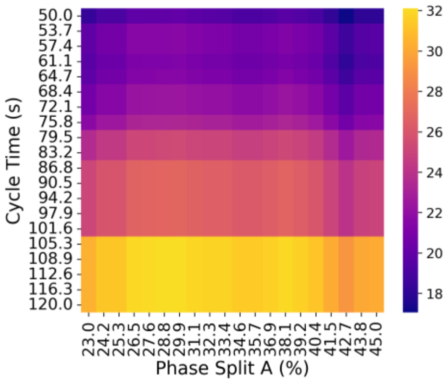

(c)

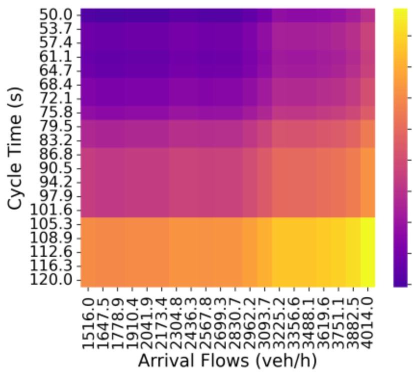

(d)

Figure 12. Heatmap for the interaction of (a) cycle time and phase split C, (b) cycle time and phase split B, (c) cycle time and phase split A, and (d) cycle time and arrival flow.

Figure 12c shows that control delay increases with both cycle time and Phase Split A. The observed behavior suggests that Phase A can serve a supporting role in balancing the westbound approach, where through and left-turn movements operate simultaneously. Moderate increases in green time improve local discharge conditions and partially mitigate the increase in delay under longer cycle lengths.

Figure 12d demonstrates the interaction between arrival flow and cycle length. The effect of cycle time becomes more pronounced under high demand conditions. Specifically, when arrival flow exceeds approximately 3200 veh/h and cycle lengths exceed 105 s, higher delay levels are observed, resulting in reduced operational performance under high-demand and long-cycle conditions.

Overall, the interaction pattern highlights the combined role of signal timing and traffic demand in shaping delay at signalized intersections, emphasizing the importance of jointly optimizing cycle length and phase split allocation in signal timing design. Furthermore, the direction and magnitude of the interaction vary according to the traffic movements served by each phase. While increasing green time for the major east-west movements (Phase B) generally reduce delay, excessive allocation to turning movements represented by Phase C tends to increase overall intersection delay. These findings confirm that delay at signalized intersections is primarily the outcome of interacting with operational parameters rather than the independent effect of any single variable.

These interaction-based insights are effectively captured through the XAI-based modeling framework, which provides an understanding of the relationship between signal control parameters, traffic demand, and intersection delay. By treating traffic delay as a data-driven indicator of operational inefficiency, the model enables an assessment of which signal control parameters drive delay and efficiency and supports data-driven signal control strategies under varying demand conditions.

Conclusion

The proposed EBM-based framework captures nonlinear relationships between traffic demand, signal timing parameters, and intersection delay while providing interpretable insights into traffic performance. Compared with established benchmark models, including Random Forest and XGBoost, the EBM model achieves comparable predictive accuracy while offering enhanced interpretability through global importance, shape functions, and interaction analysis.

The results indicate that cycle time and phase split allocation are among the primary influential factors affecting delay formation, while interaction effects reveal that their influence is strongly dependent on traffic demand conditions. Phase B (major east-west movements) generally reduces delay when adequately prioritized, whereas excessive allocation to Phase C (turning movements) may increase overall intersection delay. Moreover, the effect of cycle length becomes more pronounced under higher demand levels, indicating distinct operational regimes rather than a single optimal signal timing setting.

The findings also suggest that effective traffic signal control may be better represented through operational ranges rather than single optimal parameter values. Excessive green time allocation to one phase may reduce the efficiency of competing phases and increase delay, highlighting the need for balanced signal timing strategies under varying traffic conditions. Finally, the comparative analysis indicates that although RF and XGBoost provide good predictive performance, the EBM framework achieves a useful balance between prediction accuracy and interpretability, making it particularly suitable for traffic engineering applications.

The interpretation results provided by the EBM model can offer practical decision support for transportation agencies and traffic engineers. By identifying the relative importance of traffic demand and signal timing variables, as well as their nonlinear effects and interactions on intersection delay, the proposed approach can assist in prioritizing signal timing adjustments, evaluating alternative timing strategies, and supporting more informed operational decision-making.

The proposed approach was developed and evaluated based on SIDRA-generated scenarios for a three-leg signalized intersection. The scenario design covers a range of traffic demand and signal timing conditions under a controlled simulation environment with a constant base saturation flow rate. The results are interpreted within the context of the proposed framework. The analysis is based on 50 generated scenarios, which provide a representative set of operational conditions for delay analysis. Future research may extend the proposed framework to different intersection geometries and field-observed datasets, as well as explore larger and more diverse scenario sets to further improve model generalizability. In addition, comparative studies with alternative machine learning approaches and real-time implementation within traffic management systems may enhance practical applicability.

Ethics committee approval and conflict of interest statement

There is no need to obtain permission from the ethics committee for the article prepared.

There is no conflict of interest with any person / institution in the article prepared.

Authors' Contributions

Authors make contributions to conception and design, acquisition of data, and analysis and interpretation of data.

References

[1] Z. Cakici and Y. S. Murat, "A differential evolution algorithm-based traffic control model for signalized intersections," *Advances in Civil Engineering,* vol. 2019, no. 7360939, pp. 1-16, 2019, doi: 10.1155/2019/7360939.

[2] A. I. M. Almadi, R. E. Al Mamlook, Y. Almarhabi, I. Ullah, A. Jamal, and N. Bandara, "A Fuzzy-Logic Approach Based on Driver Decision-Making Behavior Modeling and Simulation," *Sustainability,* vol. 14, no. 14, p. 8874, 2022, doi: 10.3390/su14148874.

[3] R. Carillo, F. Cerasuolo, G. Bovenzi, D. Ciuonzo, and A. Pescapè, "Explainable federated class incremental learning for Encrypted Network Traffic classification," *Computer Networks,* vol. 269, p. 111448, 2025, doi: 10.1016/j.comnet.2025.111448.

[4] A. P. Akgüngör and E. Korkmaz, "Analysis and Modelling of the Relationship between Stopped and Control Delays by Differential Evolution Algorithm," *The Open Civil Engineering Journal,* vol. 10, no. 1, pp. 266-279, 2016, doi: 10.2174/1874149501610010266.

[5] HCM, "Highway Capacity Manual," Washington, D.C. :Transportation Research Board, 2000.

[6] F. V. Webster, "Traffic signal settings, road research technical paper No: 39," *Road Research Laboratory, London,* 1958.

[7] Akçelik, R., "Traffic Signals: Capacity and Time Analysis, Australian Road Research Board, Research Report ARR No.123," 1981.

[8] S. P. Çalışkanelli, F. Atasever Coşkun, and S. Tanyel, "Start-up Lost Time and its Effect on Signalized Intersections in Turkey," *Traffic&Transportation,* vol. 29, no. 3, pp. 321-329, 2017.

[9] M. Çetin and Y. Ş. Murat, "Doygun Akımın Belirlenmesinde Sürücü Davranışına Bağlı Bir Matematik Yaklaşım," *İMO Teknik Dergi,* vol. 24, no. 117, pp. 6399-6414, 2013.

[10] Y. Ş. Murat and Ö. Baskan, "Modeling vehicle delays at signalized junctions: Artificial neural networks approach," *Journal of Scientific & Industrial Research,* vol. 65, pp. 558-564, 2006.

[11] E. Doğan, A. P. Akgüngör, and T. Arslan, "Estimation of delay and vehicle stops at signalized intersections using artificial neural network," *Engineering Review,* vol. 36, no. 2, pp. 157-165, 2016.

[12] P. Ranpura, V. Shukla, and R. Gujar, "Estimation of vehicle control delay using artificial intelligence techniques for heterogeneous traffic conditions," *Expert Systems with Applications,* vol. 246, p. 123206, 2024, doi: 10.1016/j.eswa.2024.123206.

[13] M. E. C. Bagdatli and A. S. Dokuz, "Vehicle Delay Estimation at Signalized Intersections Using Machine Learning Algorithms," *Transportation Research Record: Journal of the Transportation Research Board,* vol. 2675, no. 9, pp. 110-126, 2021, doi: 10.1177/03611981211036874.

[14] Y. Ş. Murat, "Comparison of fuzzy logic and artificial neural networks approaches in vehicle delay modeling," *Transportation Research Part C: Emerging Technologies,* vol. 14, no. 5, pp. 316-334, 2006, doi: 10.1016/j.trc.2006.08.003.

[15] A. Mahmoudian, M. Bypour, and M. Kioumarsi, "Explainable Boosting Machine Learning for Predicting Bond Strength of FRP Rebars in Ultra High-Performance Concrete," *Computation,* vol. 12, no. 202, pp. 1-35, 2024, doi: 10.3390/computation12100202.

[16] H. Wang, Y. Ding, Y. Kong, D. Sun, Y. Shi, and X. Cai, "Predicting the Compressive Strength of Sustainable Portland Cement–Fly Ash Mortar Using Explainable Boosting Machine Learning Techniques," *Materials,* vol. 17, no. 4744, pp. 1-21, 2024, doi: 10.3390/ma17194744.

[17] Z. Liu *et al.*, "Nonlinear Cooling Effect of Street Green Space Morphology: Evidence from a Gradient Boosting Decision Tree and Explainable Machine Learning Approach," *Land,* vol. 11, no. 2220, pp. 1-23, 2022, doi: 10.3390/land11122220.

[18] I. Ahmed, I. Kumara, V. Reshadat, A. S. M. Kayes, W.-J. van den Heuvel, and D. A. Tamburri, "Travel Time Prediction and Explanation with Spatio-Temporal Features: A Comparative Study," *Electronics,* vol. 11, no. 1, p. 106, 2021, doi: 10.3390/electronics11010106.

[19] X. Zhang, "Traffic Flow Prediction Based on Explainable Machine Learning," *Highlights in Science, Engineering and Technology,* vol. 56, pp. 56-64, 2023, doi: 10.54097/hset.v56i.9816.

[20] R. Alahmadi, H. Almujibah, S. Alotaibi, A. E. A. Elshekh, M. Alsharif, and M. Bakri, "Explainable Boosting Machine: A Contemporary Glass-Box Model to Analyze Work Zone-Related Road Traffic Crashes," *Safety,* vol. 9, no. 4, p. 83, 2023, doi: 10.3390/safety9040083.

[21] W.-L. Liu, J. Zhong, P. Liang, J. Guo, H. Zhao, and J. Zhang, "Towards explainable traffic signal control for urban networks through genetic programming," *Swarm and Evolutionary Computation,* vol. 88, no. 101588, 2024, doi: 10.1016/j.swevo.2024.101588.

[22] P. Santhiya *et al.*, "Explainable artificial intelligence for traffic signal detection using LIME algorithm," *International Journal of Informatics and Communication Technology (IJ-ICT),* vol. 13, no. 3, p. 527, 2024, doi: 10.11591/ijict.v13i3.pp527-536.

[23] K. M. Erten and R. Gürfidan, "Regression-Based Performance Prediction in Asphalt Mixture Design and Input Analysis with SHAP," *Applied Sciences,* vol. 15, no. 19, p. 10779, 2025, doi: 10.3390/app151910779.

[24] C. O. Retzlaff *et al.*, "Post-hoc vs ante-hoc explanations: xAI design guidelines for data scientists," *Cognitive Systems Research,* vol. 86, p. 101243, 2024, doi: 10.1016/j.cogsys.2024.101243.

[25] D. Erol and Ö. Başkan, "Developing a Capacity Model for Roundabouts Using SIDRA Calibrated via Simulation-Based Optimization," *Sustainability,* vol. 17, no. 10289, 2025, doi: 10.3390/su172210289.

[26] P. Çalişkanelli and S. Tanyel, "Investigating the driver's response time at signalized intersections," *Transport,* vol. 33, no. 2, pp. 380-388, 2016, doi: 10.3846/16484142.2016.1250106.

[27] C. Ng, S. Susilawati, and I. C. Mei Leng, "Piecewise Linear Regression: A Statistical Method for the Analysis of the Relationship between Traffic Signal Parameters and Air Pollutant Emissions," in *Australasian Transport Research Forum 2016 Proceedings*, Melbourne, Australia, November, 16 – 18, 2016, 2016.

[28] H. K. An *et al.*, "Optimized Intersection Signal Timing: An Intelligent Approach-Based Study for Sustainable Models," *Sustainability,* vol. 14, no. 18, p. 11422, 2022, doi: 10.3390/su141811422.

[29] Akçelik & Associates. "SIDRA Glossary of Road Traffic Analysis Terms." https://www.sidrasolutions.com/learn/glossary (accessed Jan 20, 2026).

[30] E. Doğan and A. P. Akgüngör, "Optimizing a fuzzy logic traffic signal controller via the differential evolution algorithm under different traffic scenarios," *Simulation,* vol. 92, no. 11, pp. 1013-1023, 2016, doi: 10.1177/0037549716673217.

[31] E. Korkmaz and A. P. Akgüngör, "Optimizing of phase plan, sequence and signal timing based on flower pollination algorithm for signalized intersections," *Soft Computing,* vol. 25, no. 6, pp.

4243-4259, 2020, doi: 10.1007/s00500-020-05438-x.

[32] E. Korkmaz and A. P. Akgüngör, "Comparison of artificial bee colony and flower pollination algorithms in vehicle delay models at signalized intersections," *Neural Computing and Applications,* vol. 32, no. 8, pp. 3581-3597, 2018, doi: 10.1007/s00521-018-3670-3.

[33] Z. Cakici and G. Aksoy, "Does the minimization of the average vehicle delay and the minimization of the average number of stops mean the same at the signalized intersections?," *International Journal of Transportation Science and Technology,* vol. 13, pp. 213-228, 2024, doi: 10.1016/j.ijtst.2024.01.003.

[34] A. A. Assolie, N. S. A. Sukor, I. Khliefat, and T. S. B. Abd Manan, "Modeling of Queue Detector Location at Signalized Roundabouts via VISSIM Micro-Simulation Software in Amman City, Jordan," *Sustainability,* vol. 15, no. 11, p. 8451, 2023, doi: 10.3390/su15118451.

[35] T. R. Currin, *Introduction to Traffic Engineering: A Manual for Data Collection and Analysis*, 2nd Edition ed. Cengage Learning, 2012.

[36] J. Wu, X. Jin, and A. J. Horowitz, "Methodologies for Estimating Vehicle Queue Length at Metered On-Ramps," *Transportation Research Record: Journal of the Transportation Research Board,* vol. 2047, no. 1, pp. 75-82, 2008, doi: 10.3141/2047-09.

[37] A. Bozkurt and P. Çalışkanelli, "Investigation The Effects of One Way/Two Way Applications on Signalized Intersection Performance," presented at the 2. International European Conference on Interdisciplinary Scientific Researches, Ankara, July 4-5, 2020.

[38] A. Bozkurt, "İzmir Kent Merkezindeki Trafik Yönetimi Uygulamalarının Başarımlarının İrdelenmesi," Master Thesis, Civil Engineering, Transportation, Dokuz Eylul University, Graduate School of Natural and Applied Sciences, 2021.

[39] S. Mosharafian, S. Afzali, and J. Mohammadpour Velni, "Leveraging autonomous vehicles in mixed-autonomy traffic networks with reinforcement learning-controlled intersections," *Transportation Letters,* pp. 1-12, 2022, doi: 10.1080/19427867.2022.2146302.

[40] K. Culik, A. Kalasova, P. Fabian, and J. Ondrus, "Enhancing Intersection Efficiency: A Comparative Analysis of Converting Single-Lane Roundabout to Turbo Roundabout," *Sensors,* vol. 25, no. 22, p. 7002, 2025, doi: 10.3390/s25227002.

[41] B. Şişman, G. Sarisoy, and Y. Delice, "Katlı Kavşak Düzenleme Önerilerinde Simülasyon Programı Kullanım Sürecinin İrdelenmesi," *Afyon Kocatepe University Journal of Sciences and Engineering,* vol. 21, no. 6, pp. 1434-1452, 2021, doi: 10.35414/akufemubid.931834.

[42] A. E. Maxwell, M. Sharma, and K. A. Donaldson, "Explainable Boosting Machines for Slope Failure Spatial Predictive Modeling," *Remote Sensing,* vol. 13, no. 24, p. 4991, 2021, doi: 10.3390/rs13244991.

[43] C. Banyong *et al.*, "Machine Learning-Based Analysis of Travel Mode Preferences: Neural and Boosting Model Comparison Using Stated Preference Data from Thailand's Emerging High-Speed Rail Network," *Big Data and Cognitive Computing,* vol. 9, no. 6, p. 155, 2025.

[44] A. Khattak, J. Zhang, P.-W. Chan, F. Chen, and H. Almujibah, "Explainable Boosting Machine: A Contemporary Glass-Box Strategy for the Assessment of Wind Shear Severity in the Runway Vicinity Based on the Doppler Light Detection and Ranging Data," *Atmosphere,* vol. 15, no. 1, pp. 1-19, 2024, doi: 10.3390/atmos15010020.

[45] X. Zhang, L. Wu, Z. Li, and H. Liu, "A Robust Method to Measure the Global Feature Importance of Complex Prediction Models," *IEEE Access,* vol. 9, pp. 7885-7893, 2021, doi: 10.1109/ACCESS.2021.3049412.

[46] W. Alajali, W. Zhou, S. Wen, and Y. Wang, "Intersection Traffic Prediction Using Decision Tree Models," *Symmetry,* vol. 10, no. 9, p. 386, 2018, doi: 10.3390/sym10090386.

[47] A. Alsahaf, N. Petkov, V. Shenoy, and G. Azzopardi, "A framework for feature selection through boosting," *Expert Systems with Applications,* vol. 187, p. 115895, 2022, doi: 10.1016/j.eswa.2021.115895.

[48] D. M. Vlachogiannis, S. Moura, and J. Macfarlane, "Intersense: An XGBoost model for traffic regulator identification at intersections through crowdsourced GPS data," *Transportation Research Part C: Emerging Technologies,* vol. 151, p. 104112, 2023, doi: 10.1016/j.trc.2023.104112.

[49] X. Li, P. Xu, and Y.-J. Wu, "Pedestrian crossing volume estimation at signalized intersections

using Bayesian additive regression trees," *Journal of Intelligent Transportation Systems,* vol. 26, no. 5, pp. 557-571, 2021, doi: 10.1080/15472450.2021.1933471.

[50] D. Herzalla, W. T. Lunardi, and M. Andreoni, "TII-SSRC-23 Dataset: Typological Exploration of Diverse Traffic Patterns for Intrusion Detection," *IEEE Access,* vol. 11, pp. 118577-118594, 2023, doi: 10.1109/access.2023.3319213.

[51] Z. Chen and W. Fan, "A Freeway Travel Time Prediction Method Based on an XGBoost Model," *Sustainability,* vol. 13, no. 15, p. 8577, 2021, doi: 10.3390/su13158577.

[52] X. Zhang and Q. Zhang, "Short-Term Traffic Flow Prediction Based on LSTM-XGBoost Combination Model," *Computer Modeling in Engineering & Sciences,* vol. 125, no. 1, pp. 95-109, 2020, doi: 10.32604/cmes.2020.011013.

[53] L. Zhu, S. Shu, L. Zou, and M. Fernandez-Veiga, "XGBoost-Based Travel Time Prediction between Bus Stations and Analysis of Influencing Factors," *Wireless Communications and Mobile Computing,* vol. 2022, no. 3504704, pp. 1-25, 2022, doi: 10.1155/2022/3504704.

[54] I. Betkier and M. Oszczypała, "A novel approach to traffic modelling based on road parameters, weather conditions and GPS data using feedforward neural networks," *Expert Systems with Applications,* vol. 245, p. 123067, 2024, doi: 10.1016/j.eswa.2023.123067.

[55] X. Lu, C. Chen, R. Gao, and Z. Xing, "Prediction of High-Speed Traffic Flow around City Based on BO-XGBoost Model," *Symmetry,* vol. 15, no. 1453, pp. 1-17, 2023, doi: 10.3390/sym15071453.

[56] A. Korner *et al.*, "Explainable Boosting Machine approach identifies risk factors for acute renal failure," *Intensive Care Med Exp,* vol. 12, no. 1, p. 55, Jun 14 2024, doi: 10.1186/s40635-024-00639-2.